



# Group X phospholipase A<sub>2</sub> is released during sperm acrosome reaction and controls fertility outcome in mice

Jessica Escoffier,<sup>1,2</sup> Ikram Jemel,<sup>3,4</sup> Akemi Tanemoto,<sup>5</sup> Yoshitaka Taketomi,<sup>5,6</sup> Christine Payre,<sup>3,4</sup> Christelle Coatrieux,<sup>3,4</sup> Hiroyasu Sato,<sup>5,6</sup> Kei Yamamoto,<sup>6</sup> Seiko Masuda,<sup>5,6</sup> Karin Pernet-Gallay,<sup>1,2</sup> Virginie Pierre,<sup>1,2</sup> Shuntaro Hara,<sup>5</sup> Makoto Murakami,<sup>5,6,7</sup> Michel De Waard,<sup>1,2</sup> Gérard Lambeau,<sup>3,4</sup> and Christophe Arnoult<sup>1,2</sup>

<sup>1</sup>Grenoble Institute of Neuroscience, INSERM U836, Grenoble, France. <sup>2</sup>Université Joseph Fourier, Grenoble, France.

<sup>3</sup>Institut de Pharmacologie Moléculaire et Cellulaire, CNRS — UMR 6097, Valbonne, France. <sup>4</sup>Université de Nice–Sophia Antipolis, Valbonne, France.

<sup>5</sup>Department of Health Chemistry, School of Pharmaceutical Sciences, Showa University, Tokyo, Japan. <sup>6</sup>Biomembrane Signaling Project, The Tokyo Metropolitan Institute of Medical Science, Tokyo, Japan. <sup>7</sup>PRESTO, Japan Science and Technology Agency, Saitama, Japan.

**Ejaculated mammalian sperm must undergo a maturation process called capacitation before they are able to fertilize an egg. Several studies have suggested a role for members of the secreted phospholipase A<sub>2</sub> (sPLA<sub>2</sub>) family in capacitation, acrosome reaction (AR), and fertilization, but the molecular nature of these enzymes and their specific roles have remained elusive. Here, we have demonstrated that mouse group X sPLA<sub>2</sub> (mGX) is the major enzyme present in the acrosome of spermatozoa and that it is released in an active form during capacitation through spontaneous AR. mGX-deficient male mice produced smaller litters than wild-type male siblings when crossed with mGX-deficient females. Further analysis revealed that spermatozoa from mGX-deficient mice exhibited lower rates of spontaneous AR and that this was associated with decreased *in vitro* fertilization (IVF) efficiency due to a drop in the fertilization potential of the sperm and an increased rate of aborted embryos. Treatment of sperm with sPLA<sub>2</sub> inhibitors and antibodies specific for mGX blocked spontaneous AR of wild-type sperm and reduced IVF success. Addition of lysophosphatidylcholine, a catalytic product of mGX, overcame these deficiencies. Finally, recombinant mGX triggered AR and improved IVF outcome. Taken together, our results highlight a paracrine role for mGX during capacitation in which the enzyme primes sperm for efficient fertilization and boosts premature AR of a likely phospholipid-damaged sperm subpopulation to eliminate suboptimal sperm from the pool available for fertilization.**

## Introduction

Spermatogenesis within the testis leads to the production of morphologically mature sperm that are still functionally immature, immotile, and incompetent for fertilization. Before fertilization, sperm should undergo two major series of important morphological, biochemical, and functional modifications, one within the epididymis and the other within the female reproductive tract after ejaculation. During their transit through the epididymis, sperm acquire progressive motility and prime the signaling pathways that will eventually orchestrate capacitation. The full fertilization potential of spermatozoa will be reached *in vivo* only after capacitation, a final maturation process occurring in the female reproductive tract. Capacitation was discovered by Austin and Chang in the early 1950s and is defined as a complex set of molecular events that allow ejaculated sperm to fertilize an egg (1, 2). Fertilization then starts with sperm binding on the zona pellucida (ZP), followed by the physiological acrosome reaction (AR), which is essential for sperm-oocyte fusion. Only fully capacitated spermatozoa can bind to the zona-intact egg and are competent for AR (3). However, during capacitation, a large fraction of sperm (30%–40%) undergoes a premature AR called spontaneous AR (4). This process is currently interpreted as a sperm malfunction and suggests that a subpopula-

tion of ejaculated sperm does not tolerate the above-described final maturation process. The endogenous factors responsible for spontaneous AR and the possible physiological reasons for this process have not been identified. Indeed, the molecular mechanisms of sperm capacitation are still poorly understood, even after 50 years of intensive research (5–10). If capacitation clearly depends on cellular redox activity, ion fluxes, and protein phosphorylations, this process is also characterized by a strong dependence on the lipid membrane composition and lipid metabolism. Indeed, major lipid remodeling events of sperm including reorganization of the plasma membrane and formation of membrane subdomains, have been observed during capacitation at both chemical and biophysical levels (10, 11). During capacitation, the most well-known modification of the plasma membrane is cholesterol efflux, which plays a major role in sperm maturation both *in vivo* and *in vitro* (5). Other major changes during capacitation include remodeling of lipid rafts, efflux of desmosterol, and changes in sterol sulfates, phospholipids, sphingomyelin, and ceramides, all of them likely contributing to the increase in membrane fluidity by changing lipid packing and thereby providing heterogeneity of the sperm population (5, 12–14). If several families of lipolytic enzymes are involved in these lipid modifications (15), phospholipases A<sub>2</sub> (PLA<sub>2</sub>s) are likely to be important, because of their abundant expression in male reproductive organs (16–19) and because of their great diversity of action, from phospholipid remodeling and lipid mediator release to inflammation and host defense (20, 21).

**Authorship note:** Gérard Lambeau and Christophe Arnoult are co-senior authors.

**Conflict of interest:** The authors have declared that no conflict of interest exists.

**Citation for this article:** *J Clin Invest.* 2010;120(5):1415–1428. doi:10.1172/JCI40494.



PLA<sub>2</sub>s catalyze the hydrolysis of phospholipids at the *sn*-2 position to generate free fatty acids and lysophospholipids, which are precursors of different lipid mediators, such as eicosanoids and platelet-activating factor (PAF) (23, 23). PLA<sub>2</sub> metabolites either leave the cellular membrane and are involved in different cellular signaling pathways or accumulate in the leaflet of the membrane and change its biophysical properties. PLA<sub>2</sub>s constitute one of the largest families of lipid-hydrolyzing enzymes and have been classified into several groups (20). Based on their respective structure and cellular localization, PLA<sub>2</sub>s can be divided into 2 major sets of proteins: a set of 15 distinct Ca<sup>2+</sup>-dependent and Ca<sup>2+</sup>-independent intracellular PLA<sub>2</sub>s and another set of 10 Ca<sup>2+</sup>-dependent secreted PLA<sub>2</sub>s (sPLA<sub>2</sub>s). The PLA<sub>2</sub> family also includes a set of intracellular and secreted forms of PAF acetylhydrolase. Deciphering the biological functions of each PLA<sub>2</sub> member is challenging. Studies over the last decade have shown that intracellular PLA<sub>2</sub>s and extracellular PLA<sub>2</sub>s are involved in the production of various lipid mediators in different tissues and cell types, these lipid mediators being important in numerous and diverse physiological and pathophysiological conditions (21–24).

Several intracellular and secreted PLA<sub>2</sub>s in the testis and other male reproductive organs have been described, but their respective functions in reproduction still remain largely obscure. Group VIII B PAF acetylhydrolase and group VIA calcium-independent PLA<sub>2</sub> (iPLA<sub>2</sub>β) have been found in sperm, and the corresponding deficient mice present defects in early spermatogenesis and sperm motility, respectively (17, 18, 25). Previous studies have also shown that several sPLA<sub>2</sub>s including group IIA, IIC, IID, IIE, IIF, V, and X are present in various genital male organs, such as testis, epididymis, vas deferens, seminal vesicles, and prostate, but their exact functions are still speculative (16, 26). More particularly, mouse group IIE, V, and X sPLA<sub>2</sub>s (mGIIE, mGV, and mGX, respectively) have been localized in spermatogenic cells, but their presence in mature sperm and their specific functions in capacitation and/or fertilization remain to be determined.

Irrespective of the above, different studies have shown that one or several uncharacterized PLA<sub>2</sub>s play an important role in capacitation, AR, and the early steps of fertilization, including sperm binding and sperm-oocyte fusion (19). First, several biochemical studies have demonstrated the presence of one or several low-molecular-weight Ca<sup>2+</sup>-dependent sPLA<sub>2</sub>-like proteins in spermatozoa from different species, yet their molecular nature still remains elusive (27–29). As for capacitation, a spontaneous release of PAF during capacitation has been linked to activation of spontaneous AR, but the enzyme responsible for PAF release has not been identified (30). As for AR, induction of AR using nonphysiological and physiological stimuli such as Ca<sup>2+</sup> ionophore, progesterone, and ZP produces the release of arachidonic acid and/or lysophosphatidylcholine (LPC) and is prevented by PLA<sub>2</sub> inhibitors on sperm from various species (31–34). However, the identity of the PLA<sub>2</sub>(s) involved in this exocytotic event has not yet been revealed, and the use of poorly specific PLA<sub>2</sub> inhibitors such as Ro-31-4493, aristolochic acid, or ONO RS-82 in these studies cannot provide any clue (31, 33, 34). PLA<sub>2</sub> activation during AR is also supported by the fact that LPC and fatty acids accelerate or promote exocytosis (35, 36). Finally, LPC improves sperm binding on ZP (37) and sperm-oocyte fusion (38), supporting the notion that one or several PLA<sub>2</sub>s including an sPLA<sub>2</sub> protein may be important for capacitation and fertilization.

In this study, we have used mouse group X sPLA<sub>2</sub>-deficient mice (referred to herein as mGX<sup>-/-</sup> mice), sPLA<sub>2</sub> inhibitors, and recom-

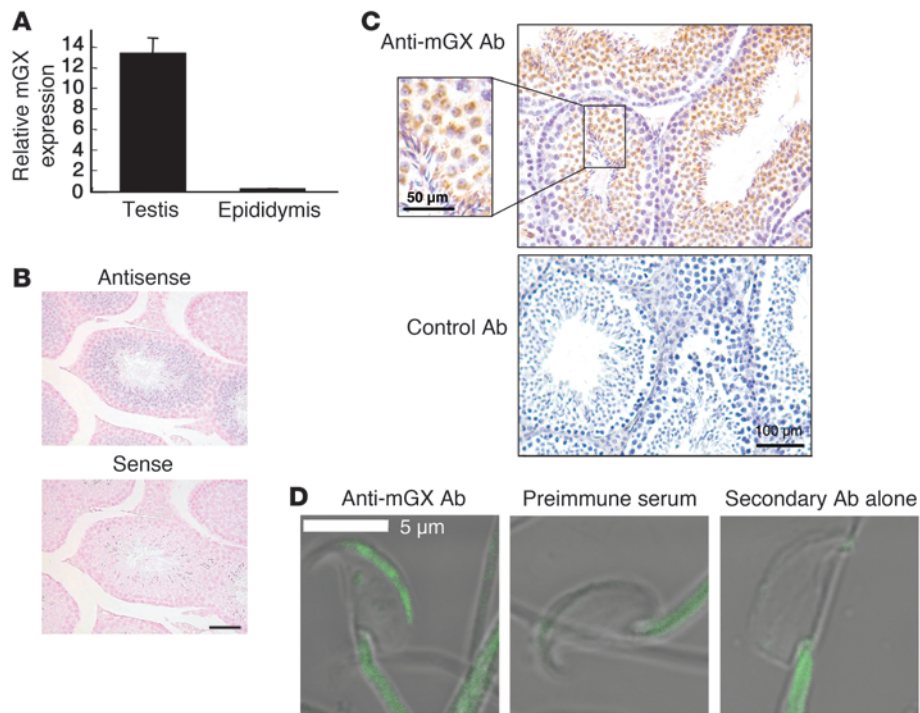
binant mGX protein to identify what we believe to be a novel role of this particular sPLA<sub>2</sub>. We demonstrated that mGX sPLA<sub>2</sub> is the major enzyme present in the acrosome of mature spermatozoa and is released as an active enzyme during AR. mGX controls sperm physiology at two levels: first, during capacitation, by triggering spontaneous AR of a specific subpopulation of sperm; and second, during the subsequent fertilization by improving the sperm fertilization potential.

In a companion to the present article, Sato et al. (39) show that another enzyme, the mouse group III sPLA<sub>2</sub>, is highly expressed in the proximal epithelium of epididymis and that mice deficient for this sPLA<sub>2</sub> exhibit male infertility because of profound defects in sperm maturation within the epididymis. Together, our results show that two catalytically active sPLA<sub>2</sub>s are expressed in different locations within the reproductive male organs and exert nonredundant functions at two major steps of maturation of spermatozoa — during their transit through the epididymis and during capacitation — with important impacts on male fertility in both cases.

## Results

*mGX sPLA<sub>2</sub> is specifically expressed in late spermatogenic cells and in the acrosome of mature spermatozoa.* Quantitative RT-PCR analysis showed that the mRNA coding for mGX is present at much higher levels in the testis than epididymis (Figure 1A). Furthermore, in situ hybridization on tissue sections of the testis from 8-week-old C57BL/6J mice showed that mGX mRNA is present in late spermatogenic cells (spermatocytes and spermatids, but not spermatogonia) in the seminiferous tubules (Figure 1B). In accordance with these results, immunohistochemistry experiments on parallel tissue sections with a specific polyclonal mGX antibody showed the presence of mGX in spermatocytes and spermatids, but not in spermatogonia (Figure 1C). In magnified views (Figure 1C, inset), scattered signals with crescent and elongated shapes were evident in spermatocytes and spermatids, suggesting that mGX is localized in the acrosomal area. In human testis, immunohistochemistry experiments showed that group X sPLA<sub>2</sub> was also present in spermatocytes and spermatids (Supplemental Figure 1A; supplemental material available online with this article; doi:10.1172/JCI40494DS1), in contrast to group IIF and V sPLA<sub>2</sub>s, which were present at different locations (Supplemental Figure 1, B and C). To further support the acrosomal location of mGX sPLA<sub>2</sub>, spermatozoa from caudae epididymis were stained with anti-mGX or control antibodies. A strong and specific immunofluorescent signal for mGX was confined to the sperm head, and more particularly in the acrosomal crescent zone (Figure 1D).

*mGX sPLA<sub>2</sub> is released during AR.* To further demonstrate that mGX is an acrosomal protein, we monitored its release from mouse mature sperm undergoing in vitro capacitation in conditions known to induce spontaneous AR of 30%–40% of the sperm population over a 90-minute incubation time. The presence of mGX and other sPLA<sub>2</sub>s possibly found in the acrosome was first determined using specific and sensitive (down to 5 pg per assay for mGX) time-resolved fluoroimmunoassays (TR-FIAs) recently developed for the different mouse sPLA<sub>2</sub>s (40). Our experiments demonstrated that the amount of mGX protein was increased in the supernatant, with a concomitant decrease in the pellet during capacitation (Figure 2A). Moreover, inducing AR by the Ca<sup>2+</sup> ionophore A23187 resulted in a 2.5-fold increase in the amount of mGX released at 90 minutes of capacitation. Remarkably, the sum amount of mGX was constant during capacitation, showing

**Figure 1**

Expression of mGX sPLA<sub>2</sub> in mouse spermatogenic cells. **(A)** Quantitative RT-PCR analysis shows that mGX mRNA is expressed in the testis, but only minimally in the epididymis. **(B)** In situ hybridization. Sections of testis from 8-week-old C57BL/6J mice were hybridized with antisense and sense probes for mGX. Positive signal for mGX was detected in spermatogenic cells (spermatocytes and spermatids, but not spermatogonia) in the seminiferous tubules. Original magnification,  $\times 200$ . Scale bar: 100  $\mu\text{m}$ . **(C)** Immunohistochemistry. Sections of the testis from 8-week-old C57BL/6J mice were stained with anti-mGX antibody or control antibody. Intense staining was found in spermatocytes and spermatids in the seminiferous tubules but not in spermatogonia (original magnification,  $\times 200$ ). In magnified views, scattered signals with crescent and elongated shapes were evident in spermatocytes and spermatids, suggesting labeling in the acrosomal area. **(D)** Spermatozoa from caudae epididymis were stained with anti-mGX antibody or control antibodies. Immunofluorescent signal for mGX sPLA<sub>2</sub> was confined to the sperm head. Note that the staining along the tail was nonspecific, since sperm treated with preimmune serum or only secondary antibody were also stained.

the accuracy of our measurements in supernatants and pellets (Figure 2A). The fact that mGX redistributed from the pellet to the supernatant during capacitation or after A23187-induced AR clearly demonstrates that the enzyme is present in the acrosome of mature sperm. When mGX<sup>-/-</sup> sperm were used in similar capacitation experiments, no mGX TR-FIA signal was detected, validating the specificity of the results (Figure 2B). We also examined the presence of other sPLA<sub>2</sub>s including mGIIA, mGIID, mGIIE, mGIIF, and mGV in the sperm of various mouse strains (C57BL/6J, BALB/c, and OF1), and none of these sPLA<sub>2</sub>s were detected (Supplemental Figure 2). We then monitored the sPLA<sub>2</sub> enzymatic activity in supernatant and pellet during capacitation by a sensitive sPLA<sub>2</sub> enzymatic assay utilizing radiolabeled *E. coli* membranes as a substrate. In accordance with the mGX sPLA<sub>2</sub> TR-FIA data, the sPLA<sub>2</sub> enzymatic activity was increased in the supernatant and decreased in the pellet (Figure 2C). The respective increases and decreases in sPLA<sub>2</sub> activity during capacitation were entirely due to mGX, since only barely detectable and constant levels of enzymatic activity were measured with mGX<sup>-/-</sup> sperm (Figure 2D). The fact that the sPLA<sub>2</sub> activity specifically released during capacitation was due

to mGX sPLA<sub>2</sub> was further confirmed by inhibition with an antibody raised against mGX, with no effect of antibodies raised against mGIIA or mGIIF (Figure 2E). Finally, the enzymatic activity was of an sPLA<sub>2</sub> type, but not cytosolic PLA<sub>2</sub> (cPLA<sub>2</sub>) or iPLA<sub>2</sub> $\beta$ , since these latter enzymes are known to be inactive on *E. coli* membranes (41, 42) and since the measured PLA<sub>2</sub> activity was fully blocked by EDTA, DTT, and LY329722 (Figure 2E), which are broad but specific inhibitors of sPLA<sub>2</sub>s (43, 44). Parallel experiments performed with recombinant mGX protein and the above inhibitors further demonstrate that mGX is responsible for most of the sPLA<sub>2</sub> enzymatic activity in supernatant and pellet (Figure 2E). Together, these results demonstrate that mGX is the major sPLA<sub>2</sub> present in the acrosome of mature mouse sperm, that the enzyme is released during AR in an active form, and that it contributes to most if not all of the sPLA<sub>2</sub> enzymatic activity released in the sperm bathing medium during capacitation.

*Disruption of the Pla2g10 gene coding for mGX sPLA<sub>2</sub> results in an impaired fertility outcome.* Although no obvious reproductive phenotype has been reported for mGX<sup>-/-</sup> male mice (45, 46), we reinvestigated this point by studying the fertility outcome in natural mating and in vitro fertilization (IVF) experiments. Both male and female mGX<sup>-/-</sup> mice were fertile when mated with WT littermate C57BL/6J mice (Figure 3A). However, the average litter size of mGX<sup>-/-</sup> male mice crossed with mGX<sup>-/-</sup>

females ( $5.70 \pm 0.42$  pups,  $n = 10$ ,  $P < 0.01$ ) was slightly lower than that of WT littermates ( $7.75 \pm 0.49$  pups,  $n = 37$ ) (Figure 3A), suggesting a lower fertility of mGX<sup>-/-</sup> animals. Because of the large amount of mGX in the sperm acrosome, we reinvestigated the role of mGX in sperm by performing IVF with mGX<sup>-/-</sup> sperm and WT oocytes. We scored the different types of egg/oocytes obtained 24 hours after mixing sperm with oocytes: unfertilized oocytes, 2-cell embryos (normal stage), and aborted embryos; and we used the 2-cell embryo values to measure fertility (47), since 2-cell embryos are appropriate for transfer into the female tract (Figure 3, B and C). As a control, we confirmed that oocytes incubated without sperm in M16 medium for 24 hours did not present any type of cell division (data not shown). In IVF experiments, the fertilizing potential of mGX<sup>-/-</sup> sperm was clearly impaired when compared with that of WT littermate sperm (Figure 3D). Indeed, the rate of 2-cell embryos was reduced from  $67.6\% \pm 2.2\%$  ( $n = 13$ ) to  $37.6\% \pm 3.9\%$  ( $n = 11$ ,  $P < 0.01$ ) for mGX<sup>+/+</sup> sperm and mGX<sup>-/-</sup> sperm, respectively. Furthermore, the rate of aborted embryos increased from  $7.7\% \pm 1.6\%$  to  $11.9\% \pm 1.9\%$  ( $n = 11$ ,  $P < 0.05$ ) for mGX<sup>+/+</sup> and mGX<sup>-/-</sup> sperm, respectively. Finally, the

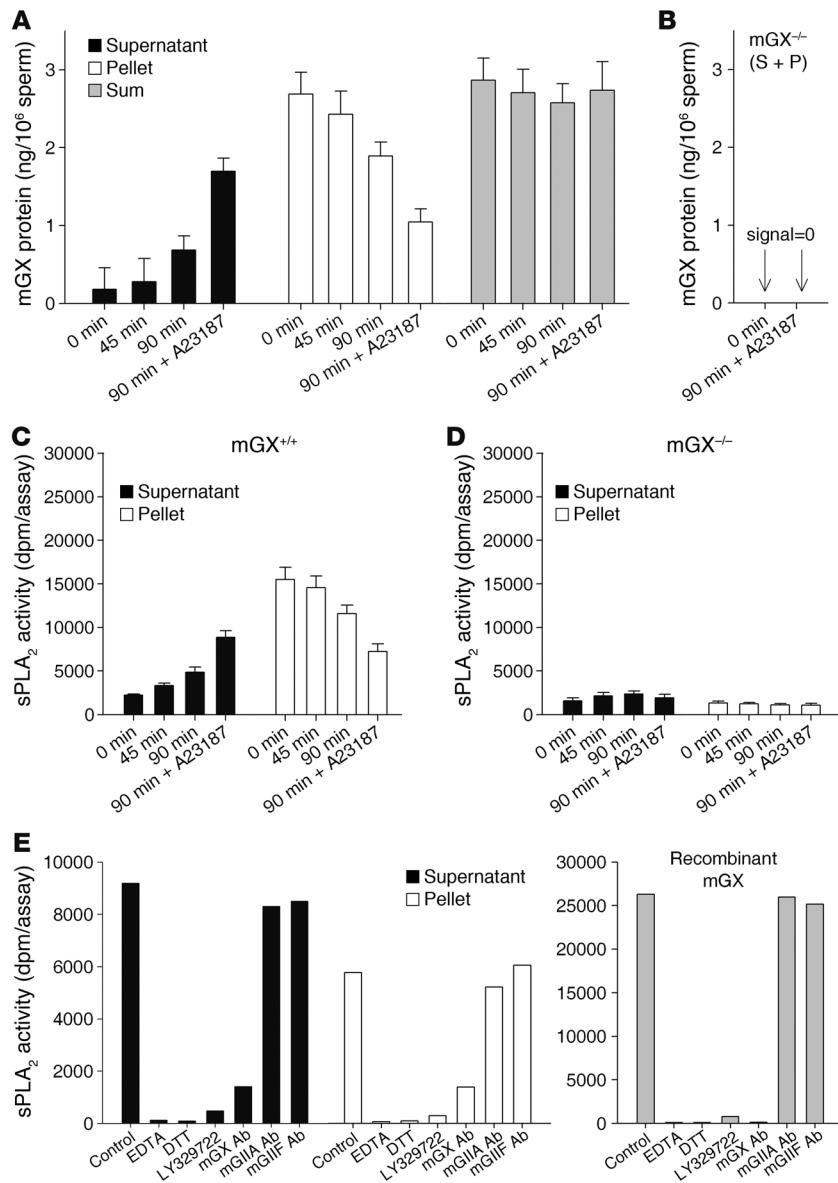


**Figure 2**

Catalytically active mGX sPLA<sub>2</sub> is released from sperm during AR. (A) Total amount of mGX protein measured by TRF-IA in supernatants and cell pellets of WT sperm during capacitation (up to 90 minutes) and after AR triggered by addition of the Ca<sup>2+</sup> ionophore A23187 (5 μM) between 60 and 90 minutes. “Sum” corresponds to the total amount of mGX in both fractions at various times. (B) Similar assays using mGX<sup>-/-</sup> sperm, showing no mGX signal (sum of supernatant and pellet [S + P]) before capacitation (0 minutes) and after A23187-induced AR. (C) Total sPLA<sub>2</sub> enzymatic activity measured using *E. coli* radiolabeled enzymatic assays in supernatants and cell pellets of WT sperm during capacitation (n = 5). (D) Similar enzymatic assays using mGX<sup>-/-</sup> sperm, showing no variation in sPLA<sub>2</sub> enzymatic activity throughout capacitation in both fractions (n = 4). (E) sPLA<sub>2</sub> enzymatic activities of supernatants and cell pellets of WT sperm (at 90 minutes + A23187) and of recombinant mGX (0.1 nM, n = 2) are inhibited by EDTA (20 mM), DTT (10 mM), LY329722 (10 μM), and anti-mGX antibody (IgG fraction, 5 μg), but not by anti-mGIIA and anti-mGIIF antibodies (n = 2).

percentage of unfertilized oocytes for mGX<sup>-/-</sup> sperm was more than 2-fold higher than that for mGX<sup>+/+</sup> sperm. Interestingly, the impaired fertility of mGX<sup>-/-</sup> sperm was rescued by a short incubation of mGX<sup>-/-</sup> sperm with recombinant mGX protein at the end of the capacitation period (Figure 3E; see also the detailed protocol of IVF with treated sperm in Supplemental Figure 3).

*Endogenous mGX sPLA<sub>2</sub> regulates spontaneous AR.* The fact that mGX sPLA<sub>2</sub> is released during AR and lysophospholipids and fatty acids, two products of sPLA<sub>2</sub>, activity can activate AR (35, 48) makes possible that the mGX released during the early time points of capacitation boosts spontaneous AR in a paracrine manner. To explore this possibility, we compared the kinetics of spontaneous AR in sperm from mGX<sup>+/+</sup> and mGX<sup>-/-</sup> mice. The early onset of spontaneous AR was unchanged between mGX<sup>+/+</sup> and mGX<sup>-/-</sup> sperm. However, the level of spontaneous AR of mGX<sup>-/-</sup> sperm occurring during the late phase of capacitation (55–90 minutes) was markedly lower than that of mGX<sup>+/+</sup> sperm (Figure 4A) and reached a plateau during the late phase of capacitation (55–90 minutes);

a statistically significant difference was found between 55 and 90 minutes of capacitation for WT sperm ( $P < 5 \times 10^{-3}$ ), while no significant difference was observed for deficient sperm ( $P = 0.94$ ). Addition of recombinant mGX in the capacitation medium of mGX<sup>-/-</sup> sperm at 80 minutes rescued a normal level of spontaneous AR at 90 minutes (Figure 4A). To confirm the involvement of mGX in spontaneous AR, we evaluated the capacity of exogenous recombinant mGX to trigger AR during capacitation (Figure 4, B and C). The mGX recombinant enzyme was highly effective on noncapacitated sperm, since concentrations as low as 0.2 nM led to a 2-fold increase in spontaneous AR, while a maximal increase in AR up to approximately 65% was observed at 500 nM (Figure 4B). Noncapacitated sperm and sperm capacitated for 90 minutes were equally sensitive to a 10-minute incubation with mGX, indicating that mGX retained the ability to induce AR throughout capacitation (Figure 4C). Together, our results demonstrate that spontaneous AR occurring during the late phase of capacitation is controlled by the secretion and paracrine activity of mGX. Our

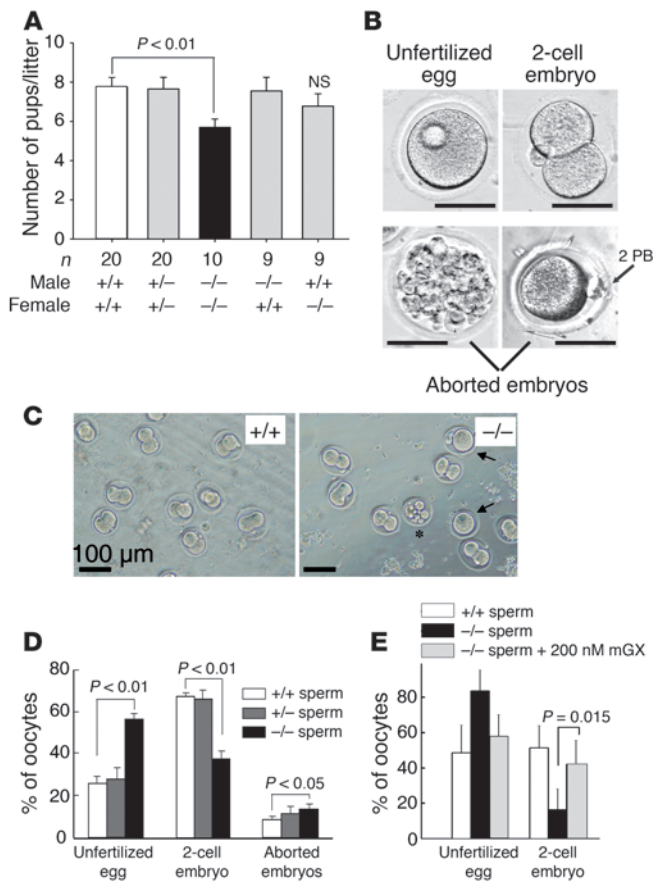


**Figure 3**

The lack of mGX sPLA<sub>2</sub> in sperm affects male fertility. **(A)** The litter sizes of intercrosses between male and female mGX-deficient mice are lower than those of littermate WT mice. Note that male and female mGX<sup>-/-</sup> mice produced normal litter size when mated with WT C57BL/6J mice **(B)** Pictures of the different stages obtained after IVF at 24 hours: unfertilized oocytes; 2-cell embryos (normal development); aborted embryos corresponding to oocytes with either multiple and uncontrolled divisions or presenting a second polar body (2 PB) but no cell division (arrows). Scale bars: 50  $\mu$ m. **(C)** Images of embryo development 24 hours after fertilization: +/+, WT sperm crossed with WT oocytes; -/-, mGX<sup>-/-</sup> sperm crossed with WT oocytes; arrows show unfertilized oocytes and asterisks show aborted embryos. **(D)** IVFs performed with mGX<sup>-/-</sup> sperm and WT oocytes have a lower rate of 2-cell embryos and higher rate of aborted embryos compared with IVFs performed with sperm from WT (+/+) or heterozygous (+/-) littermates and WT oocytes (n = 11). **(E)** The low fertilizing potential of mGX<sup>-/-</sup> sperm is rescued by recombinant mGX. IVF was performed by mixing WT oocytes with (a) WT sperm from littermates (n = 4); (b) mGX<sup>-/-</sup> sperm (n = 4); or (c) mGX<sup>-/-</sup> sperm briefly treated with 200 nM mGX (treatment for 10 minutes at the end of the capacitation period [gray bars, n = 4]). The development of eggs was evaluated after 24 hours by counting the different stages.

results also indicate that mGX modifies the ratio between two sperm subpopulations: the acrosome-reacted and the non-acrosome-reacted sperm. Importantly, we observed that very high concentrations of recombinant mGX sPLA<sub>2</sub> did not induce AR of the entire sperm population. Indeed, about 35% of the noncapacitated sperm population remained fully resistant to mGX when treated for 10 minutes, while about 18% of sperm remained resistant to mGX treatment when first capacitated for 90 minutes.

mGX sPLA<sub>2</sub> triggers AR via its catalytic activity and independently of cytosolic Ca<sup>2+</sup> rise. To determine whether the catalytic activity of mGX is required for the induction of AR, we first tested the catalytically inactive H48Q mutant of mGX, which has less than 0.1% of WT catalytic activity (49). This mutant was unable to trigger AR of noncapacitated sperm (Figure 5A). We then tested the effect of recombinant pro-mGX, the zymogen form of mGX, which has very low enzymatic activity (50). Pro-mGX was also unable to trigger AR at 500 nM (Figure 5A). Finally, we tested LY329722, a specific sPLA<sub>2</sub> inhibitor (compound A in ref. 44), and found that this inhibitor blocked the sPLA<sub>2</sub>-induced AR of capacitated sperm at 1  $\mu$ M (Figure 5B). Together, these results demonstrate that the catalytic activity of mGX is essential for inducing AR. We also wondered whether Ca<sup>2+</sup> influx was required for mGX-induced AR. To address this question, sperm were loaded during 30 minutes in a noncapacitating medium with BAPTA-AM, a cell-permeant and fast chelator of Ca<sup>2+</sup>, known to block cytosolic Ca<sup>2+</sup> increase and AR induced by ZP3 (51). Sperm were then washed and incubated for another 30 minutes to allow for a complete de-esterification of BAPTA-AM. At the end of this procedure, sperm were immobile, indicating effi-

cient chelation of cytoplasmic Ca<sup>2+</sup> by BAPTA. Sperm were then incubated with mGX for 10 minutes and scored for AR. The effect of mGX was not prevented by BAPTA, indicating that calcium signaling is not involved in sPLA<sub>2</sub>-induced AR (Figure 5C).

Acrosome-reacted and non-acrosome-reacted sperm treated with mGX sPLA<sub>2</sub> present a normal ultrastructural morphology. The subpopulation of sperm that is resistant to mGX-dependent AR is obviously the one that can fertilize eggs. This is because only non-acrosome-reacted sperm can bind to the egg and cross the ZP. It thus appeared important to check the ultrastructural integrity of the acrosome of sperm resistant to mGX treatment by electron microscopy. We found that non-acrosome-reacted sperm treated for 10 minutes with 200 nM mGX (Figure 6A) presented ultrastructural characteristics that were indistinguishable from those of untreated sperm (Figure 6B), without any apparent defect in the acrosomal area. We next analyzed the morphology of acrosome-reacted sperm. There are 3 morphological criteria by which an AR can be evaluated as normal: (a) the outer acrosomal membrane should present vesiculation; (b) the plasma membrane should fuse with the outer acrosomal membrane; and (c) the fused membrane should present a characteristic double-hairpin shape at the base of the acrosome (52). We compared A23187-induced and mGX-induced AR. All the sperm that were acrosome reacted by A23187 presented a complete AR exhibiting the 3 above morphological criteria (data not shown). The sperm that were acrosome reacted by mGX were judged as normal on the basis of the same criteria (Figure 6C). We also observed very early stages of AR-like cavitation of the acrosomal matrix (Figure 6D). Together, our analyses indicate

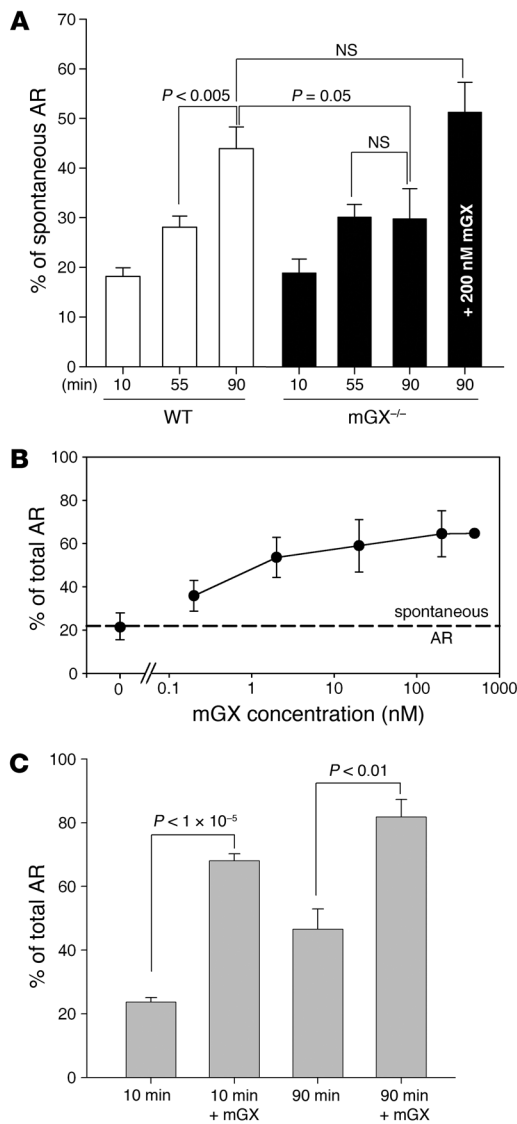


**Figure 4**

Endogenous and recombinant mGX sPLA<sub>2</sub> both regulate spontaneous AR during capacitation. **(A)** Spontaneous AR of mGX<sup>-/-</sup> sperm does not progress beyond 55 minutes of in vitro capacitation, in contrast to WT sperm. Addition of mGX during the last 10 minutes of 90-minute capacitation rescues normal spontaneous AR in mGX<sup>-/-</sup> sperm. Spontaneous AR was quantified during capacitation at 10, 55, and 90 minutes in mGX<sup>+/+</sup> littermate sperm (*n* = 11) and mGX<sup>-/-</sup> sperm (*n* = 6). **(B)** Recombinant mGX sPLA<sub>2</sub> is a potent inducer of AR. Dose-response curve for AR of noncapacitated WT sperm triggered by mGX (*n* = 3–8). **(C)** Treatment with mGX sPLA<sub>2</sub> (200 nM) for 10 minutes triggers AR of both noncapacitated WT sperm (23.7% ± 1.4% to 68.1% ± 2.1% for control and mGX-treated sperm, respectively; *n* = 23) and WT sperm capacitated for 90 minutes (46.5% ± 6.3% to 81.8% ± 5.4% for control and mGX-treated sperm, respectively; *n* = 3).

sperm with LY329722 decreased the rate of 2-cell embryos by 23% (*n* = 8, *P* = 0.023), which was compensated by an increased rate of aborted embryos (Figure 7A). Importantly, the inhibitor did not alter the fertilizing potential of sperm, since the rate of unfertilized oocytes remained constant. We also followed spontaneous AR in the presence of LY329722 during capacitation (Figure 7B). In accordance with the results obtained for mGX<sup>-/-</sup> sperm (Figure 4A), the onset of spontaneous AR was not modified by LY329722. However, the spontaneous AR occurring during the late phase of capacitation (55–90 minutes) was markedly reduced by the inhibitor. The level of spontaneous AR at 90 minutes in the presence of LY329722 was not statistically different from the level of AR of mGX<sup>-/-</sup> sperm at 90 minutes. Similar results were obtained with indoxam, another sPLA<sub>2</sub> inhibitor (50) (data not shown). Interestingly, we found that addition of 1 μM LPC, a major product of mGX sPLA<sub>2</sub> activity (43), to sperm treated with LY329722 partially rescues the level of spontaneous AR, indicating that LY329722 specifically targets mGX sPLA<sub>2</sub>. In contrast, LPC alone had no effect on spontaneous AR at this concentration (Figure 7B). Since sPLA<sub>2</sub> inhibitors such as LY329722 have a low membrane permeability (53), the inhibition of spontaneous AR is likely due to the inhibition of mGX present in the cell medium after its release, and not to inhibition of mGX still present in the acrosome. The fact that LY329722 blocks spontaneous AR and reduces 2-cell embryos (and thus fertility; see ref. 47) suggests that the level of spontaneous AR controlled by mGX is an important factor controlling the fertility outcome. To confirm this view, we performed IVF with OF1 sperm briefly treated with 200 nM recombinant mGX during the last 10 minutes of capacitation (see Supplemental Figure 3 for the time course of this experiment). In accordance with the results of Figure 4C, this treatment elicited AR of approximately 65% of treated sperm, and this effect was blocked by LY329722 (Figure 8A). This treatment led to an increased rate of 2-cell embryos from 38.09% ± 5.27% to 57.50% ± 4.69% (*n* = 13, *P* < 0.0001) for control and treated sperm, respectively (Figure 8B). Similar experiments performed with sperm and oocytes from C57BL/6J inbred mice produced an even larger increase, with a 2-fold higher rate of 2-cell embryos for mGX-treated sperm (Supplemental Figure 4). As for LY329722 (Figure 7A), mGX treatment did not change the fertilization potential of sperm, since the rate of unfertilized oocytes remained constant: the increased rate of 2-cell embryos was compensated by the decreased rate of aborted embryos (Figure 8B), from 32.95% ± 5.06% to 19.85% ± 2.96% (*n* = 13, *P* < 0.01). Furthermore, we found that embryos obtained with mGX-treated sperm

that treatment of sperm with mGX produces acrosome-reacted sperm and non-acrosome-reacted sperm with a normal morphology. The fact that the non-acrosome-reacted sperm do not appear to be damaged and have an intact acrosome indicates that it is this subpopulation of sperm that fertilizes eggs.

The fertility outcome is dependent on the rate of spontaneous AR controlled by mGX sPLA<sub>2</sub>. A fraction of the sperm population was found to be fully resistant to recombinant mGX, even at concentrations as high as 500 nM (Figure 4B). This suggests that recombinant mGX specifically targets a subpopulation of sperm and triggers their AR prematurely, i.e., before fertilization. Since endogenous mGX is released during capacitation (Figure 2), a similar mechanism may be operating physiologically, and the role of endogenous mGX would be to target a specific subpopulation of sperm that may have defective sperm function. To address this hypothesis, we performed IVF experiments with WT sperm and oocytes from outbred OF1 animals. Outbred mice were first chosen because inbred mice, and more particularly C57BL/6 mice, present a subfertile phenotype that may interfere with the results. Sperm were pretreated with the sPLA<sub>2</sub> inhibitor LY329722 throughout capacitation. Treating

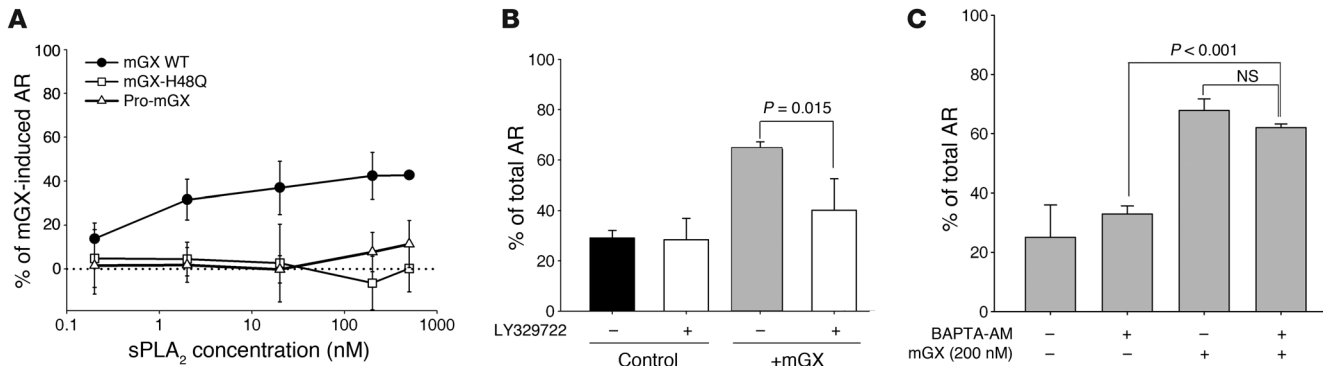


**Figure 5** mGX sPLA<sub>2</sub> triggers AR via its catalytic activity and independently of cytosolic Ca<sup>2+</sup> rise. **(A)** Dose-response curves for AR of noncapacitated sperm triggered by mGX (*n* = 3–8), mGX-H48Q (*n* = 3), and pro-mGX (*n* = 3). Results are expressed as sPLA<sub>2</sub>-specific AR, i.e., total AR minus spontaneous AR. **(B)** The specific sPLA<sub>2</sub> inhibitor LY329722 (1 μM) blocked the ability of 200 nM mGX to trigger AR of sperm capacitated during 45 minutes (*n* = 3). Results correspond to total AR. **(C)** Loading sperm with 10 μM BAPTA did not modify spontaneous AR (2 left bars, *n* = 3) and mGX-induced AR (2 right bars, *t* test; NS; *n* = 3) of sperm incubated in a noncapacitating medium (no BSA). In the presence of BAPTA-AM, the difference in the level of AR between nontreated and mGX-treated sperm is statistically significant.

developed normally to the blastocyst stage (Figure 8C) and that reimplanted blastocyst embryos gave rise to normal pups (data not shown). The effect of exogenous mGX on fertility was dependent on its enzymatic activity, since preincubation of mGX with LY329722 for 15 minutes before the short treatment of sperm prevented the positive effect on IVF (Figure 8D). We then reasoned that mGX may influence fertility by decreasing the number of sperm able to cross the ZP, and thus by decreasing the risk of polyspermy. Indeed, the number of sperm in an IVF droplet greatly exceeded the minimal number necessary to maximize the IVF outcome. To test this hypothesis, we evaluated the IVF outcome (2-cell embryos) with a

concentration of non-acrosome-reacted sperm equivalent to that obtained after mGX treatment. At a sperm concentration of  $3 \times 10^5$ , treating sperm with 200 nM mGX led to a drop in the number of non-acrosome-reacted sperm from  $2.1 \times 10^5$  (70% of  $3 \times 10^5$  cells) to  $0.9 \times 10^5$  (30% of  $3 \times 10^5$  cells); percent values are shown in Figure 8A. This drop was mimicked by performing IVF either at  $1.5 \times 10^5$  or  $3 \times 10^5$  sperm, and this dilution did not increase the fertility rate (Figure 8E). This result ruled out the hypothesis of a decreased risk of polyspermy due to mGX treatment. Together, the results shown in Figures 7 and 8 clearly indicate that the fertility outcome of our IVF experiments is linked to the level of AR controlled by mGX.

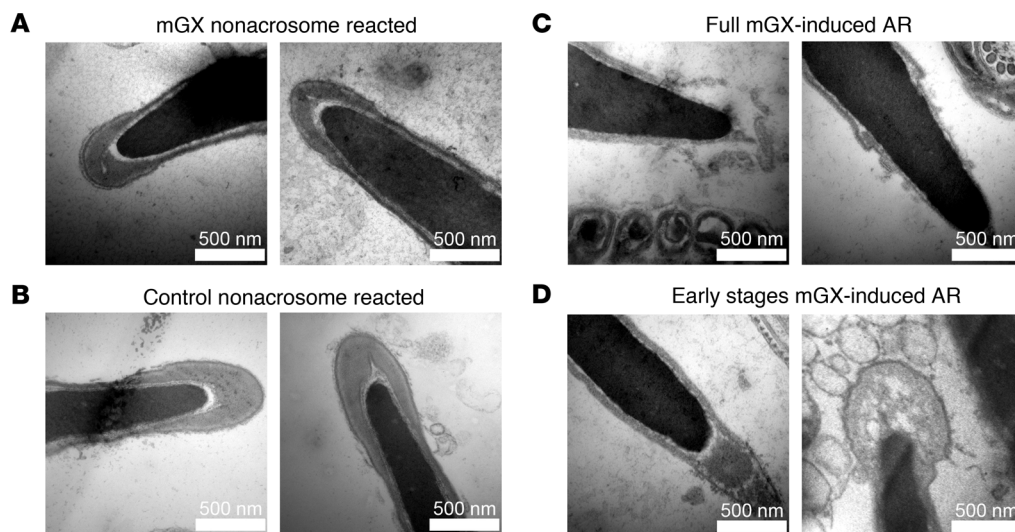


**Figure 6** Ultrastructure of the head of mGX sPLA<sub>2</sub>-treated sperm. **(A)** Electron micrographs of non-acrosome-reacted sperm treated with 200 nM mGX (noncapacitated sperm). **(B)** Electron micrographs of non-acrosome-reacted control (untreated) sperm (noncapacitated sperm). **(C)** Acrosome-reacted sperm (noncapacitated sperm) in the presence of 200 nM mGX presented normal morphological features of sperm undergoing AR: fusion between the plasma and acrosomal membrane produced vesiculation (left), and the outer acrosomal membrane was fused with the plasma membrane and presented a typical double-hairpin shape at the base of the acrosome (right) or **(D)** presented early stages of AR, i.e., cavitation. Scale bars: 500 nm.

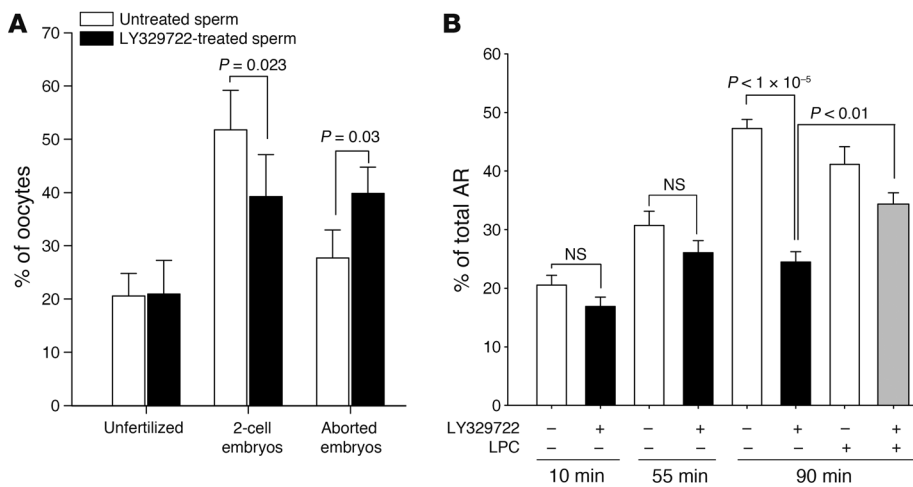


**Figure 7** Blocking endogenous mGX sPLA<sub>2</sub> with the specific inhibitor LY329722 impacts both fertility outcome and spontaneous AR. (A) Endogenous mGX, secreted during spontaneous AR, controls the yield of viable embryos, without changing the rate of fertilization. IVF experiments were performed with either control sperm or the same sperm treated throughout capacitation with 1 μM LY329722 (n = 8) and unfertilized oocytes. Two-cell embryos and aborted embryos were scored. Inhibiting mGX decreases 2-cell embryos and increases aborted embryos. The design of the experiment clearly indicates that LY329722 controls the yield of viable embryos by inhibiting endogenous mGX secreted during spontaneous AR. (B) The sPLA<sub>2</sub> inhibitor LY329722 blocked the late phase of spontaneous AR. Spontaneous AR was quantified during capacitation at 10, 55, and 90 minutes in the absence or presence of 1 μM LY329722 (n = 10–14). Incubation of sperm with 1 μM LPC during the last 45 minutes partially rescued the inhibition of spontaneous AR induced by LY329722 (n = 7).

LPC, an sPLA<sub>2</sub> metabolite, increases the fertilization potential of sperm. We have demonstrated above that mGX, which is spontaneously released by sperm during capacitation, triggers AR of a subpopulation of sperm via a paracrine amplification loop. Our IVF experiments further support the notion that this subpopulation of sperm is less fertile and poorly promotes normal embryo development. Moreover, mGX<sup>-/-</sup> sperm also present a deficit of fertilization potential, as indicated by the decrease in fertilization rate (Figure 3D). This observation is suggestive of a second role for mGX or its catalytic products downstream of capacitation, i.e., during fertilization. To test this hypothesis, we allowed WT sperm to capacitate in the presence of YM26734, another potent sPLA<sub>2</sub> inhibitor (54), then washed the sperm by centrifugation to remove the inhibitor, and finally performed IVF experiments in the absence or presence of LPC, a major catalytic product of mGX (55). Interestingly, treatment with YM26734 alone decreased the rate of 2-cell embryos by 40%, from 58.9% ± 6.8% to 35.6% ± 5.7% (n = 3). Furthermore, addition of LPC could rescue the fertilization potential of YM26734-pre-treated sperm, with a 2-cell embryo rate of 52.7% ± 9.7% (n = 3) (Figure 9A). To confirm the effect of YM26734, we performed similar experiments in the presence of an mGX rabbit polyclonal antibody and obtained similar results: the 2-cell embryo rate decreased from 51.7% ± 5.2% to 32.4% ± 2.1% for control sperm and sperm treated with mGX antibody, respectively. Addition of LPC, after the capacitation of sperm treated with the antibody, rescued the 2-cell embryo rate up to 57.1% ± 8.2% (n = 3) (Figure 9B). Importantly, we observed that treatment of sperm with LPC alone had no effect on the rate of fertilization at this concentration (data not shown). This result demonstrates that LPC, an

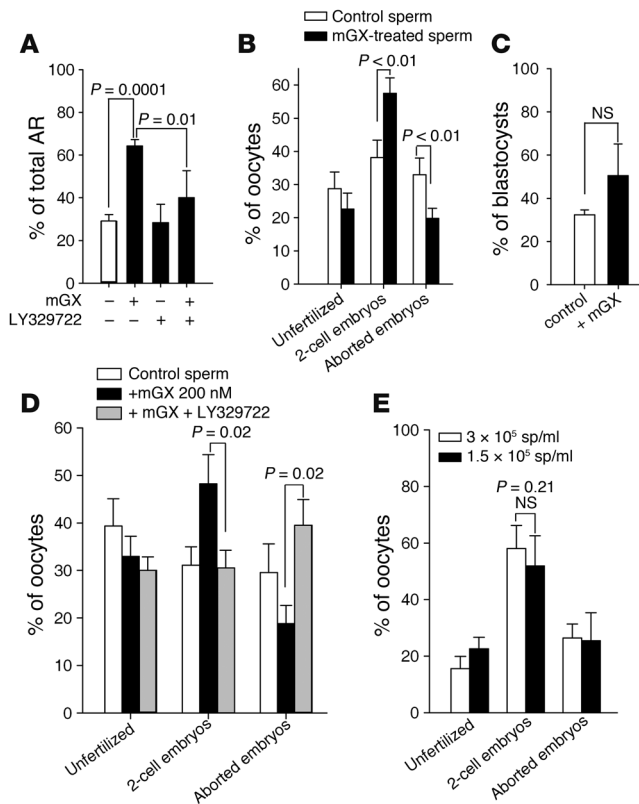
mGX metabolite, is required for normal fertilization and suggests a second role for mGX, in addition to its role in the control of spontaneous AR. The fertilization potential of the non-acrosome-reacted sperm subpopulation is thus dependent on mGX enzymatic activity, and mGX or its downstream metabolic products including LPC are likely involved in one of the different steps of fertilization occurring after capacitation, including sperm binding on ZP, ZP-induced AR, and/or sperm-egg fusion.

### Discussion

This study shows for the first time to our knowledge that mGX sPLA<sub>2</sub> is present in large amounts in the sperm acrosome and plays an important paracrine role in the control of spontaneous AR during capacitation, which is associated with a strong impact on fertility outcome. Our results also provide indirect evidence that mGX plays a role during the downstream fertilization step and thus likely acts at two major stages of reproduction, capacitation and fertilization. Finally, our findings may open new possibilities for the improvement of assisted reproduction techniques.

We first unambiguously identified mGX as the major sPLA<sub>2</sub> enzyme loaded in the mouse sperm acrosome. Although several sPLA<sub>2</sub>s are present in mouse male reproductive organs (16), we did not detect mGIIA, mGIID, mGIIE, mGIIF, and mGV sPLA<sub>2</sub> proteins in mature mouse sperm, while the expression of mGX was very high, with several nanograms of mGX protein per million sperm. This value appears very high when compared with the level of mGX protein in various mouse tissues (56) and fits with the very high level of mGX mRNA in testis versus other tissues (57). Our finding is important, since there have been numerous biochemical reports during the past 40 years showing the presence of an sPLA<sub>2</sub> protein in sperm from several mammalian species, the molecular identity of which was never clarified (19, 27–29). This unknown sPLA<sub>2</sub> was of low molecular mass; was reported as a proenzyme; was resistant to heat and acid extraction; was Ca<sup>2+</sup>-dependent; could hydrolyze both phosphatidylcholine and phosphatidylethanolamine; and was sensitive to nonspecific sPLA<sub>2</sub> inhibitors such as Mepacrine, p-bromophenacyl bromide, aristolochic acid, Ro-31-4493, and Ro-4639. Many of these features match those of group X sPLA<sub>2</sub> (43, 57, 58). The presence of group X sPLA<sub>2</sub> in the sperm acrosome in other species including humans, however, remains to be determined. Our preliminary data obtained by RT-PCR (59) and immunohistochemistry (Supplemental Figure 1) on human testis suggest that group X sPLA<sub>2</sub> is a likely candidate, but a more thorough analysis should be performed at the protein level on purified human sperm. Interestingly, a proenzyme form was detected in human sperm (28), and this would fit with human group X sPLA<sub>2</sub>, which has a propeptide sequence (58). More recently, the presence and release of an sPLA<sub>2</sub> from human sperm has been





reported (29, 38), but the two studies were performed using antibodies with unclear specificity toward the different sPLA<sub>2</sub> isoforms and were thus inconclusive regarding the identity of the human sperm sPLA<sub>2</sub>. Finally, there is evidence suggesting that other PLA<sub>2</sub>s including iPLA<sub>2</sub> $\beta$  and likely a cPLA<sub>2</sub> member are present in sperm (18, 19). The locations of these intracellular PLA<sub>2</sub>s and their likely distinct roles in sperm function remain to be investigated using inhibitors specifically targeting these enzymes.

We then investigated the role of mGX during *in vitro* capacitation and found that the sPLA<sub>2</sub> controls to a large extent the percentage of sperm undergoing “spontaneous” or premature AR, thereby inactivating them for the fertility race. Our experiments with WT versus mGX-deficient sperm indicate a delayed paracrine effect of endogenous mGX sPLA<sub>2</sub> on the rate of spontaneous AR (Figure 4A). Since different lipid mediators such as prostaglandin E<sub>1</sub> and PAF can trigger AR and are produced at the onset of *in vitro* capacitation (30, 60), it is tempting to speculate that such lipid mediators are produced by an intracellular PLA<sub>2</sub>-dependent mechanism in a subpopulation of “excessively primed” or damaged sperm, trigger initial AR, and release mGX sPLA<sub>2</sub>, which in turn amplifies spontaneous AR in a paracrine loop of activation. Recombinant mGX sPLA<sub>2</sub> can promote AR at low nM concentrations and over the entire time course of capacitation (Figure 4, B and C), demonstrating its high potency in AR. Interestingly, the effect of mGX reaches a plateau (Figure 4B) and leaves intact a subpopulation of sperm showing a normal morphology (Figure 6) and capable of fertilizing oocytes (Figure 8). Together, our results indicate that mGX makes an important contribution during *in vitro* capacitation, at least by triggering AR in a subpopulation of likely damaged sperm. This suggests a role of mGX in sperm cell sorting during capacitation as a mechanism to improve fertility

## Figure 8

Exogenous mGX sPLA<sub>2</sub> reinforces the effect of endogenous mGX on spontaneous AR and improves fertility outcome. (A) Sperm used for IVF and briefly pretreated with exogenous mGX present a higher rate of spontaneous AR. WT sperm were incubated during the last 10 minutes of capacitation with mGX alone (200 nM), LY329722 alone (1  $\mu$ M), or mGX preincubated with LY329722. Only mGX treatment triggered significant AR over the untreated condition ( $n = 6$ ). (B) Recombinant mGX controls the yield of viable embryos, without changing the rate of fertilization. IVF was performed either with OF1 control sperm or with the same sperm briefly treated with 200 nM mGX, and IVF outcome was scored ( $n = 13$ ). Recombinant mGX increases 2-cell embryos and decreases aborted embryos. (C) Two-cell embryos obtained with mGX-treated sperm developed normally to the blastocyst stage. (D) LY329722 blocks the mGX-dependent increase in fertility. IVF was performed with either control sperm or the same sperm treated briefly with 200 nM mGX or with the same sperm treated briefly with 200 nM mGX or with the same sperm treated briefly with 200 nM mGX but preincubated with 1  $\mu$ M LY329722 ( $n = 6$ ). (E) The number of sperm incubated with oocytes does not impact fertility outcome. IVF was performed at 2 different concentrations: 1.5  $\times 10^5$  and 3  $\times 10^5$  sperm (sp) ( $n = 4$ ).

outcome. Our current view of the *in vivo* situation is that the heterogeneous population of ejaculated sperm becomes exposed to mGX sPLA<sub>2</sub> (and possibly other sPLA<sub>2</sub> activities) after their mixing with seminal plasma secretions and/or during their swimming through the female tract. Indirect evidence supporting this view include the facts that (a) various populations of sperm with a different lipid composition, a damaged plasma membrane, and externalization of phosphatidylserine associated with spontaneous AR have been identified (13, 14); (b) seminal plasma and female tract secretions contain endogenous PLA<sub>2</sub> regulators (26, 61–63); and

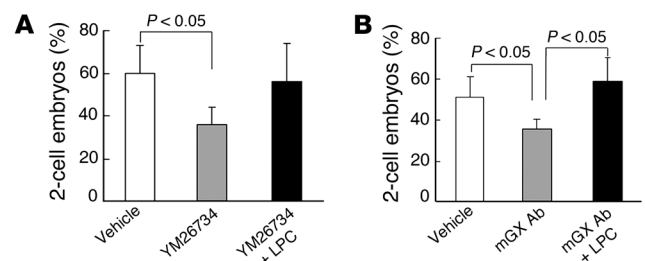


## Figure 9

Addition of LPC during fertilization rescues the fertilization potential of sperm treated with sPLA<sub>2</sub> inhibitor or anti-mGX antibody during capacitation. (A) IVF experiments were performed with sperm treated or not with the sPLA<sub>2</sub> inhibitor YM26734 (1  $\mu$ M) only during the capacitation period. LPC (1  $\mu$ g/ml) was added only during gamete mixing. The approximately 40% reduction in 2-cell embryo rate measured with YM26734-treated sperm ( $n = 3$ ,  $P < 0.05$ ) was restored by supplementation with LPC. (B) Similar reduction and recovery of IVF were observed with sperm treated with anti-mGX antibody (50  $\mu$ g/ml) during capacitation and LPC added during gamete mixing ( $n = 3$ ,  $P < 0.05$ ), respectively.



(c) a relationship was found among PLA<sub>2</sub> activity in human sperm, seminal fluid, and male fertility (64).

The mechanism by which mGX promotes AR clearly depends on its enzymatic activity, because (a) the catalytically inactive mutant H48Q and the proenzyme form of mGX are inactive and (b) the specific sPLA<sub>2</sub> inhibitor LY329722 prevents mGX-induced AR (Figure 5, A and B). The fact that the two major products of mGX sPLA<sub>2</sub>, LPC and free fatty acids, are able to trigger AR also supports this mechanism (35, 36, 48). This direct mechanism also fits with our results showing that mGX-induced AR does not require intracellular Ca<sup>2+</sup> (Figure 5C). Based on the specificity and action of group X sPLA<sub>2</sub> on different cells (43, 65), the phospholipid targets of mGX on sperm are likely phosphatidylcholine, phosphatidylethanolamine, and phosphatidylserine, especially those enriched in polyunsaturated fatty acids at the *sn*-2 position. Such phospholipids are present in caudae epididymal sperm and reorganized into microdomains in the sperm head plasma membrane during capacitation (10, 11, 66–69). The fact that about 30% of the sperm population is insensitive to mGX sPLA<sub>2</sub> while the other 70% is gradually sensitive (Figure 4) is likely related to the heterogeneous lipid nature of the sperm plasma membrane producing various subpopulations of sperm with different levels of cholesterol, lipid peroxidation, lipid dynamics, and phospholipid asymmetry (70). Indeed, the enzymatic activity of group X sPLA<sub>2</sub> has been shown to be influenced by the lipid composition of the plasma membrane, notably by the ratio between sphingolipids and phosphatidylcholine species (71). Furthermore, it has been shown that the enzymatic activity of several sPLA<sub>2</sub>s is dependent on lipid packing and phospholipid asymmetry (72). The ratio of phospholipids to sphingomyelin is changed during sperm maturation, and this is likely a way to control mGX activity on distinct sperm subpopulations. Interestingly, sphingomyelinase speeds up sperm capacitation and increases spontaneous AR (73). Whether mGX may be acting on a particular population of damaged sperm with altered plasma phospholipid asymmetry including externalized phosphatidylserine or oxidized phospholipids associated with a decreased fertility potential remains to be determined (15, 70, 74, 75).

We have clearly demonstrated that mGX sPLA<sub>2</sub> is a potent regulator of spontaneous AR during capacitation and that a defect in this process or its inhibition reduces fertility outcome by increasing the rate of aborted embryos and decreasing the rate of 2-cell embryos. We have indeed demonstrated that (a) decreasing AR by inhibition of mGX decreases fertility outcome, while increasing AR by addition of recombinant mGX increases fertility outcome; and (b) mGX<sup>-/-</sup> sperm show simultaneously a lower rate of spontaneous AR and a higher rate of aborted embryos. In sperm from CD46-deficient mice, a positive link between the rate of spontaneous AR and fertility has also been mentioned but not demonstrated (4). It is important to note that the effectors used to modify the rate of spontaneous AR have been applied only during capacitation and then washed out, and thus these effectors or mGX catalytic products are unlikely to affect the downstream fertilization events. Our experiments thus support a model whereby mGX sPLA<sub>2</sub> targets a subpopulation of sperm, triggers their premature AR during capacitation, and thereby discards them from the competition race for fertilization, since only non-acrosome-reacted sperm can cross the ZP. Therefore, the so-called spontaneous AR would correspond in part to the premature AR triggered by mGX, and the latter would represent a physiological mechanism of sperm cell sorting that compensates for the unreliability in sperm production and quality (75, 76).

Our experiments also provide evidence for a second role of mGX during fertilization, after ZP-induced AR and the release of mGX in the sperm-egg environment. Indeed, we have shown that mGX<sup>-/-</sup> sperm presented fertilization rates much lower than those of mGX<sup>+/+</sup> sperm, with mean decreases of 44%–68% (Figure 3, D and E). In comparison, blocking mGX activity during capacitation of mGX<sup>+/+</sup> sperm also produced a decrease in the fertilization rate, but smaller than that with mGX<sup>-/-</sup> sperm, with mean decreases of only 24% (with LY329722, Figure 7A), 39% (with YM26734, Figure 9A), and 37% (with mGX antibody, Figure 9B). These results clearly support a second role of mGX downstream of capacitation. Assuming that mGX has two different mechanisms of action, one during capacitation and another during fertilization, one should expect to see a more robust effect on fertility when using mGX<sup>-/-</sup> sperm than when using an sPLA<sub>2</sub> inhibitor or an antibody, which were only added during capacitation and only blocked released mGX sPLA<sub>2</sub>. Indeed, it is important to note that in the experiments using LY329722 or mGX antibody, the acrosomal mGX of non-acrosome-reacted sperm should remain fully active, since LY329722 analogs have low permeability (53), antibodies are impermeant, and these compounds were washed out before gamete mixing. The fact that addition of LPC during the fertilization step was able to restore the fertilizing potential of sperm capacitated in conditions where mGX was inhibited also supports a role of mGX when secreted during ZP-induced AR. Besides, LPC increases both sperm binding to ZP and sperm-oocyte fusion (37, 38). The targets of the mGX metabolites allowing sperm to efficiently fertilize an egg, however, remain to be determined. In conclusion, we have demonstrated that the *in vitro* fertility outcome is controlled by mGX, acting at two different stages, and any defects in mGX activity at these stages produces a drop in fertility.

We have, however, observed no defect in fertility when mGX-deficient male mice were crossed with WT females. This would argue for a noncritical role of mGX in sperm function, but given the essential role of sperm in the propagation of life, a redundancy of systems would not be unexpected. Indeed, there are many examples of knockout mice lacking important genes in sperm physiology and AR that are apparently fertile because of redundant or compensatory mechanisms. A nonexhaustive list of such genes includes Ca<sup>2+</sup> channels (77, 78), acrosin (79), caveolin-1 (80), and a sperm-specific aminophospholipid transporter (15). The lack of obvious reproductive defect in mGX<sup>-/-</sup> mice may be linked to the presence and role of multiple extra- or intracellular PLA<sub>2</sub> activities in sperm physiology that may act in concert or may be partially redundant (17–19). However, we observed a lower fertility when crossing male and female mGX-deficient mice (Figure 3). This result suggests that mGX is also present in the female tract and may compensate for the deficit of mGX in sperm. This view is supported by our preliminary data showing the presence of mGX sPLA<sub>2</sub> in the female reproductive tract, notably in the uterine epithelium (56). Similar observations have been made for iPLA<sub>2</sub>β-deficient mice, where crossings between iPLA<sub>2</sub>β-deficient males and females produced no offspring, while crossings between iPLA<sub>2</sub>β-deficient males and WT females did produce offspring, though at less than the normal rate (18). This mGX<sup>-/-</sup> sperm phenotype may be reminiscent of a well-known human infertility situation where the infertility of a couple is due to the combination of male and female deficits. Such a cause is involved in 20% of infertile couples (79).

Finally, we have demonstrated that recombinant mGX boosts the effect of endogenous mGX on spontaneous AR and signifi-



cantly improves the rate of success of IVF in the mouse species, an improvement that is even greater in inbred mice known to present a subfertile phenotype. Moreover, non-acrosome-reacted sperm that were resistant to mGX treatment showed a normal ultrastructural morphology, and the oocytes fertilized with this sperm developed normally up to the blastocyst stage *in vitro* and gave rise to normal pups when reimplanted. Thus, mGX is a peculiar sPLA<sub>2</sub> that represents a hope for new therapeutic strategies to fight against human male infertility: mGX could be used as a potent therapeutic agent in assisted reproduction techniques, either to improve IVF outcome or to select sperm for intracytoplasmic sperm injection (ICSI) based on their acrosomal status. This strategy would be based on prior treatment of the sperm population with group X sPLA<sub>2</sub> (or another relevant human sPLA<sub>2</sub>) and subsequent selection of non-acrosome-reacted sperm for IVF or ICSI.

## Methods

**Animals.** All animal procedures were performed according to French and Japanese guidelines on the use of living animals in scientific investigations with the approval of the respective local ethical review committees (the Grenoble Institut des Neurosciences ethical committee and the Institutional Animal Care and Use Committees of Showa University and of the Tokyo Metropolitan Institute of Medical Science). mGX-deficient mice (null for the *Pla2g10* gene) on a C57BL/6J background were obtained from Lexicon Inc. as described previously (45). All other animals were from Charles River Laboratories. All animals used were 2–6 months old.

**In situ hybridization.** A 355-bp DNA fragment corresponding to the nucleotide positions 221–576 of mouse cDNA (GenBank NM\_011987) was subcloned into a pGEMT-Easy vector (Promega) and was used for generation of sense or antisense RNA probes. Digoxigenin-labeled RNA probes were prepared with DIG RNA Labeling Mix (Roche). Paraffin-embedded mouse testis sections (6 µm) were obtained from Genostaff Co. For *in situ* hybridization, the sections were hybridized with digoxigenin-labeled RNA probes (300 ng/ml) at 60°C for 16 hours. The bound label was detected using NBT-BCIP, an alkaline phosphate color substrate. The sections were counterstained with Kernechtrot (Muto Pure Chemicals Co.).

**Quantitative RT-PCR.** Total RNA was isolated from testis and epididymis of 8-week-old male C57BL/6J mice with TRIzol reagent (Invitrogen) and purified using an RNeasy Purification Kit (QIAGEN). First-strand cDNA synthesis was performed using a High-Capacity cDNA Reverse Transcription Kit (Applied Biosystems). Quantitative RT-PCR analysis was carried out on an ABI Prism 7000 Sequence Detection System (Applied Biosystems) using Power SYBR Green PCR Master Mix (Applied Biosystems) and the TaqMan probe for mGX (Mm00449530\_m1). The thermal cycling conditions comprised initial steps at 50°C for 2 minutes and 95°C for 10 minutes, followed by 40 cycles of amplification at 95°C for 20 seconds, 55°C for 20 seconds, and 72°C for 30 seconds. The expression of 18S mouse ribosomal RNA (accession number X00686) was used for normalization.

**Immunohistochemistry.** Mouse testis samples were fixed in 4% PFA and embedded in paraffin. The tissue sections (4 µm thick) were incubated with Target Retrieval Solution (Dako Cytomation) as required and then incubated overnight at 4°C with rabbit anti-mGX antibody (from M.H. Gelb, University of Washington, Seattle, Washington, USA) or normal rabbit IgG at 1:100 dilution in 10 mM Tris-HCl (pH 7.4) containing 0.15 M NaCl (TBS). The sections were then treated with a catalyzed signal-amplified System Staining Kit (Dako Cytomation) with diaminobenzidine substrate, followed by counterstaining with hematoxylin and eosin. Human testis sections (from 16-year-old males) were obtained by surgery at Toho University Ohmori Hospital (Tokyo, Japan) following approval by the ethical committee of the faculty and receipt of informed consent from the patients.

**Immunofluorescence microscopy.** Epididymal spermatozoa from C57BL/6J mice were washed with PBS and fixed on glass slides with 3% (v/v) PFA in TBS for 1 hour. After 3 washes with PBS, fixed cells were treated with blocking solution (1% [w/v] bovine serum albumin and 0.5% [w/v] saponin in TBS) for 1 hour; then with rabbit anti-mGX or control antibody at 1:200 dilution in blocking solution for 2 hours; and then with FITC-conjugated anti-rabbit IgG antibody at 1:200 dilution in blocking solution for 2 hours, with 3 washes between each incubation. After 6 washes with TBS, immunofluorescent signals were visualized with a laser scanning confocal microscope (IX70; Olympus).

**Capacitation and AR assay.** Sperm from caudae epididymides were allowed to swim in M2 medium for 10 minutes. When specified, sperm were capacitated in M16 medium with 2% fatty acid-free BSA at 37°C in a 5% CO<sub>2</sub> incubator for various times. For sPLA<sub>2</sub> treatment, sperm were incubated with sPLA<sub>2</sub> in M16 medium at 37°C for the last 10 minutes. Cells were transferred in PBS solution and then fixed with 4% PFA solution for 2 minutes. Sperm were washed (100 mM ammonium acetate, 2 minutes), wet mounted on slides, and air dried. Slides were then rinsed with water and stained with Coomassie blue (0.22%) for 2 minutes and finally rinsed. Slides were analyzed, and at least 150 sperm were scored.

**Electron microscopy.** Sperm were fixed with 2.5% glutaraldehyde in 0.1 M Na<sup>+</sup> cacodylate pH 7.4 during 2 hours at room temperature. Cells were washed with buffer and postfixed with 1% osmium tetroxide in the same buffer for 1 hour at 4°C. After washing with water, cells were stained overnight at 4°C with 0.5% uranyl acetate pH 4.0. Cells were dehydrated through graded alcohol (30%, 60%, 90%, 100%, 100%, and 100%) and infiltrated with a mix of 1:1 Epon/alcohol 100% during 1 hour before several baths of fresh Epon (Fluka) during 3 hours. Finally, cells were centrifuged and immersed in fresh Epon and polymerized during 3 days at 60°C. Ultrathin sections of the cell pellet were cut with an ultramicrotome (Leica). Sections were post-stained with 4% uranyl acetate and 1% lead citrate before being observed in an electron microscope at 80 kV (JEOL 1200EX).

**Detection of sPLA<sub>2</sub> proteins in sperm.** Sperm from caudae epididymides of different mouse strains (mGX<sup>-/-</sup> or WT C57BL/6J littermates, OF1, and BALB/c) were allowed to swim for 15 minutes at 37°C in 2.5 ml of M2 medium. Sperm were then washed by centrifugation at 500 g twice with M2 medium, then resuspended in 2.5 ml M16 medium. Five hundred microliters of sperm were then diluted in 4.5 ml M16 medium containing 2% fatty acid-free BSA and further incubated at 37°C for 10, 45, and 90 minutes. In some assays, A23187 Ca<sup>2+</sup> ionophore (5 µM) was added between 60 and 90 minutes of incubation. After incubation, sperm were spun down for 8 minutes at 500 g, and supernatants and cell pellets were flash frozen in liquid nitrogen and stored at -80°C. sPLA<sub>2</sub> protein and enzymatic activity were analyzed on crude supernatants and cell pellets after resuspension in 500 µl M16 medium containing a cocktail of protease inhibitors (EDTA-free complete inhibitor set, Roche Biochemicals) and lysis with a Branson 350 Sonifier Cell Disruptor. TR-FIAs for sPLA<sub>2</sub> were performed as described previously with minor modifications (56). Briefly, 1–5 µl of protein sample were diluted in 100 µl of DELFIA assay buffer (Tris-HCl-buffered NaCl solution, pH 7.8, containing NaN<sub>3</sub>, BSA, bovine gamma globulins, Tween 40, DTPA, and inert red dye, PerkinElmer Wallac) and added to sPLA<sub>2</sub> IgG-coated microtiter wells previously washed twice with TR-FIA washing solution (10 mM Tris-HCl, pH 7.8, containing 0.9% NaCl, 0.04% NaN<sub>3</sub>, and 0.02% Tween 20). After incubation at room temperature with constant shaking at 200 cycles/min for 30 minutes, wells were washed 4 times with TR-FIA washing solution, incubated with 100 µl of Eu-labeled mGX IgG tracer (0.5 µg/ml diluted in DELFIA assay buffer), and washed again 4 times as above. After washing, 100 µl of DELFIA enhancement solution was added to wells and incubated at room temperature for 5 minutes with shaking at 200 cycles/min and thereafter for 10 minutes without shak-



ing. Time-resolved fluorescence was measured using a Wallac Envision PerkinElmer plate reader and optimized optical modules for DELFIA assays. sPLA<sub>2</sub> enzymatic activity was measured using radiolabeled *E. coli* membranes as substrate (43). Briefly, 5–50 µl of cell lysates or supernatants were incubated for 60 minutes in 300 µl of sPLA<sub>2</sub> activity buffer (0.1 M Tris pH 8.0, 10 mM CaCl<sub>2</sub>, and 0.1% BSA containing 100,000 dpm of [<sup>3</sup>H]oleate-radiolabeled *E. coli* membranes. Reactions were stopped by addition of 300 µl stop buffer (0.1 M EDTA pH 8.0 and 0.5% fatty acid-free BSA). Mixtures were centrifuged at 10,000 g for 5 minutes, and supernatants containing released [<sup>3</sup>H]oleate were counted.

**Production of recombinant sPLA<sub>2</sub>s and sPLA<sub>2</sub> antibodies.** Recombinant mouse group IIA, IID, IIE, IIF, V, and X sPLA<sub>2</sub>s were produced as described previously (81). Pro-mGX sPLA<sub>2</sub> and the H48Q mutant of mGX sPLA<sub>2</sub> were produced as for mature WT mGX sPLA<sub>2</sub> using the pAB3 vector, in which the nucleotide sequence coding for the propeptide and mature sequence of mGX (56) was inserted in-frame with the ΔGST protein and the factor Xa cleavage site, which were removed by cleavage with the factor Xa protease (81). Recombinant H48Q mGX and pro-mGX sPLA<sub>2</sub> were found to have 0.1% and 0.3% of WT mGX sPLA<sub>2</sub>, respectively (data not shown). All sPLA<sub>2</sub> antibodies were produced in rabbit as polyclonal antibodies raised against the different recombinant sPLA<sub>2</sub>s. The IgG fractions used above for TRF-IA and experiments depicted in Figure 2E and Figure 9 were obtained by purification on protein A-Sepharose as described previously (56).

**IVF.** Sperm, obtained by manual trituration of caudae epididymides from male mice (OF1, C57BL/6J, mGX<sup>-/-</sup> or WT littermates), were allowed to swim in M2 medium for 10 minutes. Eggs were collected from mature OF1 females (6 weeks old) synchronized with 7.5 units of pregnant mare serum gonadotrophin (PMSG) and 7.5 units of human chorionic gonadotrophin (hCG) before collection. The number of scored oocytes per condition was 43 ± 19 (min, 20; max, 109). We carried out IVF using standard protocols (82). Eggs were incubated with 1.5 × 10<sup>5</sup> to 5 × 10<sup>5</sup> sperm/ml (37°C, 5% CO<sub>2</sub>) in M16 medium for 4 hours. Unbound sperm were washed away after incubation. Twenty-four hours after fertilization, we scored the different stages (unfertilized oocytes, aborted embryos, and 2-cell embryos as an indication of successful fertilization). The schematic course of IVF experiments is presented in Supplemental Figure 3: after swimming, sperm were capacitated for 35–60 minutes in M16 2% BSA (37°C, 5% CO<sub>2</sub>). When specified, sPLA<sub>2</sub> inhibitors or mGX antibody was added during the full period of capacitation. For treatment with recombinant mGX, sperm were incubated after capacitation for the last 10 minutes in M16 medium containing 200 nM mGX (or 1 µM LY329722 or mGX plus LY329722 in some experiments). After treatment, sperm were washed by centrifugation (500 g, 5 minutes) to remove unbound drug, possible lipid metabolites, and all acrosomal compounds released during sPLA<sub>2</sub>-induced AR. The rationale for this procedure was to avoid a subsequent and uncontrolled effect on

IVF outcome by an uncharacterized compound released during AR such as PAF (30). After drug washing, the concentration of remaining unbound mGX was estimated to be lower than 1 nM, based on dilution calculation. We checked that 1 nM mGX did not induce effects on sperm-oocyte fusion (37). For this purpose, we performed IVF experiments in which sperm and oocytes were incubated with 1 nM mGX throughout capacitation and fertilization: no difference was found between control and treated gametes (data not shown). Finally, washed sperm were introduced into droplets containing between 20 and 109 oocytes. For LPC rescue experiments, LPC was introduced in the fertilization droplets at the same time as sperm. After 4 hours of incubation, unbound sperm were washed away, and IVF outcomes were scored at 24 hours.

**Chemical compounds.** M2 medium, M16 medium, and BSA (Cohn fraction V-low fatty acid) were from Sigma-Aldrich. PMSG and HCG were from CEVA Santé Animal and Intervet, respectively. LPC (L-α-LPC from chicken egg) was from Avanti and YM26734 from Yamanouchi Pharmaceuticals.

**Statistics.** Statistical analyses were performed with SigmaPlot. *t* test and paired *t* test were used to compare the effect of various compounds on AR and fertility, respectively. Data represent mean ± SEM. Statistical tests with a 2-tailed *P* values ≤ 0.05 were considered significant.

### Acknowledgments

This work was supported in part by the Région Rhône-Alpes (to C. Arnoult), CNRS (to C. Arnoult and G. Lambeau), INSERM (M. De Waard), the Association pour la Recherche sur le cancer (grant 3977) and the Agence Nationale de la Recherche (to G. Lambeau), and by grants-in aid for scientific research from the Ministry of Education, Science, Culture, Sports and Technology of Japan (to M. Murakami and S. Hara), and grants from the PRESTO program of the Japan Science and Technology Agency, the NOVARTIS Foundation for the Promotion of Science, and the Toray Science Foundation (to M. Murakami). J. Escoffier was supported by a fellowship from the Région Rhône-Alpes. We thank Lexicon Genetics Inc. for providing mGX-deficient mice and Michael Gelb for providing LY329722, indoxam, and mGX antibody. We thank H. de Pomyers and Latoxan for their support.

Received for publication July 13, 2009, and accepted in revised form February 10, 2010.

Address correspondence to: Christophe Arnoult, Grenoble Institute of Neurosciences, Equipe 3 “Calcium channels, functions and pathologies,” Bâtiment Edmond J. Safra, Site Santé à La Tronche, BP 170 38042 Grenoble Cedex 9, France. Phone: 33.4.56.52.05.64; Fax: 33.4.56.52.05.72; E-mail: christophe.arnoult@ujf-grenoble.fr.

- Austin CR. The capacitation of the mammalian sperm. *Nature*. 1952;170(4321):326.
- Chang MC. Fertilizing capacity of spermatozoa deposited into the fallopian tubes. *Nature*. 1951; 168(4277):697–698.
- Jungnickel MK, Sutton KA, Florman HM. In the beginning: lessons from fertilization in mice and worms. *Cell*. 2003;114(4):401–404.
- Inoue N, et al. Disruption of mouse CD46 causes an accelerated spontaneous acrosome reaction in sperm. *Mol Cell Biol*. 2003;23(7):2614–2622.
- Travis AJ, Kopf GS. The role of cholesterol efflux in regulating the fertilization potential of mammalian spermatozoa. *J Clin Invest*. 2002;110(6):731–736.
- Aitken RJ, Baker MA. Oxidative stress and male reproductive biology. *Reprod Fertil Dev*. 2004; 16(5):581–588.
- O’Flaherty C, De Lamirande E, Gagnon C. Positive role of reactive oxygen species in mammalian sperm capacitation: triggering and modulation of phosphorylation events. *Free Radic Biol Med*. 2006;41(4):528–540.
- Fraser LR, Adeoya-Osiguwa SA, Baxendale RW, Gibbons R. Regulation of mammalian sperm capacitation by endogenous molecules. *Front Biosci*. 2006; 11:1636–1645.
- Salicioni AM, et al. Signalling pathways involved in sperm capacitation. *Soc Reprod Fertil Suppl*. 2007;65:245–259.
- Gadella BM, Tsai PS, Boerke A, Brewis IA. Sperm head membrane reorganization during capacitation. *Int J Dev Biol*. 2008;52(5–6):473–480.
- Jones R, James PS, Howes L, Bruckbauer A, Klenerman D. Supramolecular organization of the sperm plasma membrane during maturation and capacitation. *Asian J Androl*. 2007;9(4):438–444.
- Lenzi A, Picardo M, Gandini L, Dondero F. Lipids of the sperm plasma membrane: from polyunsaturated fatty acids considered as markers of sperm function to possible scavenger therapy. *Hum Reprod Update*. 1996;2(3):246–256.
- Buffone MG, Verstraeten SV, Calamera JC, Doncel GF. High cholesterol content and decreased membrane fluidity in human spermatozoa are associated with protein tyrosine phosphorylation and functional deficiencies. *J Androl*. 2009;30(5):552–558.
- Zalata A, Hassan A, Christophe A, Comhaire F, Mostafa T. Cholesterol and desmosterol in two sperm populations separated on Sil-Select gradient [published online ahead of print March 25, 2009]. *Int J Androl*. doi: 10.1111/j.1365-2605.2009.00961.
- Wang L, Beserra C, Garbers DL. A novel aminophospholipid transporter exclusively expressed in spermatozoa is required for membrane lipid asym-



- metry and normal fertilization. *Dev Biol.* 2004; 267(1):203–215.
16. Masuda S, et al. Localization of various secretory phospholipase A2 enzymes in male reproductive organs. *Biochim Biophys Acta.* 2004;1686(1–2):61–76.
  17. Koizumi H, et al. Targeted disruption of intracellular type I platelet activating factor-acetylhydrolase catalytic subunits causes severe impairment in spermatogenesis. *J Biol Chem.* 2003;278(14):12489–12494.
  18. Bao S, et al. Male mice that do not express group VIA phospholipase A2 produce spermatozoa with impaired motility and have greatly reduced fertility. *J Biol Chem.* 2004;279(37):38194–38200.
  19. Roldan ER, Shi QX. Sperm phospholipases and acrosomal exocytosis. *Front Biosci.* 2007;12:89–104.
  20. Schaloske RH, Dennis EA. The phospholipase A2 superfamily and its group numbering system. *Biochim Biophys Acta.* 2006;1761(11):1246–1259.
  21. Lambeau G, Gelb MH. Biochemistry and physiology of mammalian secreted phospholipases A2. *Annu Rev Biochem.* 2008;77:495–520.
  22. Leslie CC. Regulation of arachidonic acid availability for eicosanoid production. *Biochem Cell Biol.* 2004;82(1):1–17.
  23. Kita Y, Ohto T, Uozumi N, Shimizu T. Biochemical properties and pathophysiological roles of cytosolic phospholipase A2s. *Biochim Biophys Acta.* 2006; 1761(11):1317–1322.
  24. Kikawada E, Bonventre JV, Arm JP. Group V secretory PLA2 regulates TLR2-dependent eicosanoid generation in mouse mast cells through amplification of ERK and cPLA2 $\alpha$  activation. *Blood.* 2007; 110(2):561–567.
  25. Yan W, Assadi AH, Wynshaw-Boris A, Eichele G, Matzuk MM, Clark GD. Previously uncharacterized roles of platelet-activating factor acetylhydrolase 1b complex in mouse spermatogenesis. *Proc Natl Acad Sci U S A.* 2003;100(12):7189–7194.
  26. Kallajoki M, Alanen KA, Nevalainen M, Nevalainen TJ. Group II phospholipase A2 in human male reproductive organs and genital tumors. *Prostate.* 1998;35(4):263–272.
  27. Thakkar JK, East J, Seyler D, Franson RC. Surface-active phospholipase A2 in mouse spermatozoa. *Biochim Biophys Acta.* 1983;754(1):44–50.
  28. Antaki P, Guerette P, Chapdelaine A, Roberts KD. Detection of pro-phospholipase A2 in human spermatozoa. *Biol Reprod.* 1989;41(2):241–246.
  29. Lessig J, Reibetanz U, Arnhold J, Glander HJ. Destabilization of acrosome and elastase influence mediate the release of secretory phospholipase A2 from human spermatozoa. *Asian J Androl.* 2008; 10(6):829–836.
  30. Wu C, et al. Evidence for the autocrine induction of capacitation of mammalian spermatozoa. *J Biol Chem.* 2001;276(29):26962–26968.
  31. Roldan ER, Fragio C. Phospholipase A2 activation and subsequent exocytosis in the Ca<sup>2+</sup>/ionophore-induced acrosome reaction of ram spermatozoa. *J Biol Chem.* 1993;268(19):13962–13970.
  32. Yuan YY, et al. Zona pellucida induces activation of phospholipase A2 during acrosomal exocytosis in guinea pig spermatozoa. *Biol Reprod.* 2003; 68(3):904–913.
  33. Pietrobon EO, Soria M, Dominguez LA, Monclus ML, Fornes MW. Simultaneous activation of PLA2 and PLC are required to promote acrosomal reaction stimulated by progesterone via G-proteins. *Mol Reprod Dev.* 2005;70(1):58–63.
  34. Shi QX, et al. Progesterone primes zona pellucida-induced activation of phospholipase A2 during acrosomal exocytosis in guinea pig spermatozoa. *J Cell Physiol.* 2005;205(3):344–354.
  35. Fleming AD, Yanagimachi R. Evidence suggesting the importance of fatty acids and the fatty acid moieties of sperm membrane phospholipids in the acrosome reaction of guinea pig spermatozoa. *J Exp Zool.* 1984;229(3):485–489.
  36. Llanos MN, Morales P, Riffo MS. Studies of lysophospholipids related to the hamster sperm acrosome reaction in vitro. *J Exp Zool.* 1993;267(2):209–216.
  37. Riffo M, Nieto A. Lysophosphatidylcholine induces changes in physicochemical, morphological, and functional properties of mouse zona pellucida interaction. *Mol Reprod Dev.* 1999;53(1):68–76.
  38. Riffo MS, Parraga M. Role of phospholipase A2 in mammalian sperm-egg fusion: development of hamster oolemma fusibility by lysophosphatidylcholine. *J Exp Zool.* 1997;279(1):81–88.
  39. Sato H, et al. Group III secreted phospholipase A2 regulates epididymal sperm maturation and fertility in mice. *J Clin Invest.* 2010;120(5):1400–1414.
  40. Nevalainen TJ, Eerola LI, Rintala E, Laine VJ, Lambeau G, Gelb MH. Time-resolved fluoroimmunoassays of the complete set of secreted phospholipases A2 in human serum. *Biochim Biophys Acta.* 2005; 1733(2–3):210–223.
  41. Kabre E, Chaib N, Boussard P, Merino G, Devleeschouwer M, Dehaye JP. Study on the activation of phospholipases A2 by purinergic agonists in rat submandibular ductal cells. *Biochim Biophys Acta.* 1999;1436(3):616–627.
  42. Marshall LA, Roshak A. Coexistence of two biochemically distinct phospholipase A2 activities in human platelet, monocyte, and neutrophil. *Biochem Cell Biol.* 1993;71(7–8):331–339.
  43. Singer AG, et al. Interfacial kinetic and binding properties of the complete set of human and mouse groups I, II, V, X, and XII secreted phospholipases A2. *J Biol Chem.* 2002;277(50):48535–48549.
  44. Smart BP, Oslund RC, Walsh LA, Gelb MH. The first potent inhibitor of mammalian group X secreted phospholipase A2: elucidation of sites for enhanced binding. *J Med Chem.* 2006;49(10):2858–2860.
  45. Henderson WR Jr, et al. Importance of group X-secreted phospholipase A2 in allergen-induced airway inflammation and remodeling in a mouse asthma model. *J Exp Med.* 2007;204(4):865–877.
  46. Fujioka D, et al. Reduction in myocardial ischemia/reperfusion injury in group X secretory phospholipase A2-deficient mice. *Circulation.* 2008; 117(23):2977–2985.
  47. Muller CH. Rationale, interpretation, validation, and uses of sperm function tests. *J Androl.* 2000; 21(1):10–30.
  48. Meizel S, Turner KO. Stimulation of an exocytotic event, the hamster sperm acrosome reaction, by cis-unsaturated fatty acids. *FEBS Lett.* 1983; 161(2):315–318.
  49. Surrel F, et al. Group X phospholipase A2 stimulates the proliferation of colon cancer cells by producing various lipid mediators. *Mol Pharmacol.* 2009;76(4):778–790.
  50. Morioka Y, et al. Mouse group X secretory phospholipase A2 induces a potent release of arachidonic acid from spleen cells and acts as a ligand for the phospholipase A2 receptor. *Arch Biochem Biophys.* 2000; 381(1):31–42.
  51. O'Toole CM, Arnoult C, Darszon A, Steinhart RA, Florman HM. Ca<sup>2+</sup> entry through store-operated channels in mouse sperm is initiated by egg ZP3 and drives the acrosome reaction. *Mol Biol Cell.* 2000; 11(5):1571–1584.
  52. Green DP. The induction of the acrosome reaction in guinea-pig sperm by the divalent metal cation ionophore A23187. *J Cell Sci.* 1978;32:137–151.
  53. Mounier CM, et al. Arachidonic acid release from mammalian cells transfected with human groups IIA and X secreted phospholipase A(2) occurs predominantly during the secretory process and with the involvement of cytosolic phospholipase A(2)- $\alpha$ . *J Biol Chem.* 2004;279(24):25024–25038.
  54. Hamaguchi K, et al. Induction of distinct sets of secretory phospholipase A(2) in rodents during inflammation. *Biochim Biophys Acta.* 2003;1635(1):37–47.
  55. Mitsuishi M, Masuda S, Kudo I, Murakami M. Human group III phospholipase A2 suppresses adenovirus infection into host cells. Evidence that group III, V and X phospholipase A2s act on distinct cellular phospholipid molecular species. *Biochim Biophys Acta.* 2007;1771(11):1389–1396.
  56. Eerola LI, Surrel F, Nevalainen TJ, Gelb MH, Lambeau G, Laine VJ. Analysis of expression of secreted phospholipases A2 in mouse tissues at protein and mRNA levels. *Biochim Biophys Acta.* 2006;1761(7):745–756.
  57. Valentin E, Ghomashchi F, Gelb MH, Lazdunski M, Lambeau G. On the diversity of secreted phospholipases A(2). Cloning, tissue distribution, and functional expression of two novel mouse group II enzymes. *J Biol Chem.* 1999;274(44):31195–31202.
  58. Cupillard L, Koumanov K, Mattei MG, Lazdunski M, Lambeau G. Cloning, chromosomal mapping, and expression of a novel human secretory phospholipase A2. *J Biol Chem.* 1997;272(25):15745–15752.
  59. Valentin E, Singer AG, Ghomashchi F, Lazdunski M, Gelb MH, Lambeau G. Cloning and recombinant expression of human group IIF-secreted phospholipase A(2). *Biochem Biophys Res Commun.* 2000; 279(1):223–228.
  60. Schaefer M, Hofmann T, Schultz G, Gudermann T. A new prostaglandin E receptor mediates calcium influx and acrosome reaction in human spermatozoa. *Proc Natl Acad Sci U S A.* 1998;95(6):3008–3013.
  61. Morishita T, Nozaki M, Sano M, Yokoyama M, Nakamura G, Nakano H. Regional differences of phospholipase A2 activity in the rabbit oviductal epithelium. *Prostaglandins Leukot Essent Fatty Acids.* 1992;47(3):199–202.
  62. Manjunath P, Soubeyrand S, Chandonnet L, Roberts KD. Major proteins of bovine seminal plasma inhibit phospholipase A2. *Biochem J.* 1994;303(pt 1):121–128.
  63. Upreti GC, Hall EL, Koppens D, Oliver JE, Vishwanath R. Studies on the measurement of phospholipase A2 (PLA2) and PLA2 inhibitor activities in ram semen. *Anim Reprod Sci.* 1999;56(2):107–121.
  64. Wang SK, Huang YF, Li BT, Xia XY, Wang ZZ. Detection and clinical significance of phospholipase A2 in semen of male infertile patients. *Zhonghua Nan Ke Xue.* 2003;9(2):90–93.
  65. Mitsuishi M, Masuda S, Kudo I, Murakami M. Group V and X secretory phospholipase A2 prevents adenoviral infection in mammalian cells. *Biochem J.* 2006;393(pt 1):97–106.
  66. Asano A, et al. Biochemical characterization of membrane fractions in murine sperm: identification of three distinct sub-types of membrane rafts. *J Cell Physiol.* 2009;218(3):537–548.
  67. Parks JE, Arion JW, Foote RH. Lipids of plasma membrane and outer acrosomal membrane from bovine spermatozoa. *Biol Reprod.* 1987;37(5):1249–1258.
  68. Thaler CD, Thomas M, Ramalje JR. Reorganization of mouse sperm lipid rafts by capacitation. *Mol Reprod Dev.* 2006;73(12):1541–1549.
  69. Wathes DC, Abayasekara DR, Aitken RJ. Polyunsaturated fatty acids in male and female reproduction. *Biol Reprod.* 2007;77(2):190–201.
  70. Silva PF, Gadella BM. Detection of damage in mammalian sperm cells. *Theriogenology.* 2006; 65(5):958–978.
  71. Singh DK, Subbaiah PV. Modulation of the activity and arachidonic acid selectivity of group X secretory phospholipase A2 by sphingolipids. *J Lipid Res.* 2007;48(3):683–692.
  72. Jensen LB, et al. Mechanisms governing the level of susceptibility of erythrocyte membranes to secretory phospholipase A2. *Biophys J.* 2005;88(4):2692–2705.
  73. Cross NL. Sphingomyelin modulates capacitation of human sperm in vitro. *Biol Reprod.* 2000; 63(4):1129–1134.
  74. Kurz A, Viertel D, Herrmann A, Muller K. Localization of phosphatidylserine in boar sperm cell membranes during capacitation and acrosome reaction. *Reproduction.* 2005;130(5):615–626.



75. de Vantery Arrighi C, Lucas H, Chardonens D, de Agostini A. Removal of spermatozoa with externalized phosphatidylserine from sperm preparation in human assisted medical procreation: effects on viability, motility and mitochondrial membrane potential. *Reprod Biol Endocrinol.* 2009;7:1.
76. Marti E, Perez-Pe R, Colas C, Muino-Blanco T, Cebrian-Perez JA. Study of apoptosis-related markers in ram spermatozoa. *Anim Reprod Sci.* 2008; 106(1-2):113-132.
77. Jungnickel MK, Marrero H, Birnbaumer L, Lemos JR, Florman HM. Trp2 regulates entry of Ca<sup>2+</sup> into mouse sperm triggered by egg ZP3. *Nat Cell Biol.* 2001;3(5):499-502.
78. Escoffier J, et al. Expression, localization and functions in acrosome reaction and sperm motility of Ca(V)3.1 and Ca(V)3.2 channels in sperm cells: an evaluation from Ca(V)3.1 and Ca(V)3.2 deficient mice. *J Cell Physiol.* 2007;212(3):753-763.
79. Nayernia K, Adham IM, Shamsadin R, Muller C, Sancken U, Engel W. Proacrosin-deficient mice and zona pellucida modifications in an experimental model of multifactorial infertility. *Mol Hum Reprod.* 2002;8(5):434-440.
80. Drab M, et al. Loss of caveolae, vascular dysfunction, and pulmonary defects in caveolin-1 gene-disrupted mice. *Science.* 2001;293(5539):2449-2452.
81. Rouault M, et al. Recombinant production and properties of binding of the full set of mouse secreted phospholipases A2 to the mouse M-type receptor. *Biochemistry.* 2007;46(6):1647-1662.
82. Fraser LR. In vitro capacitation and fertilization. *Methods Enzymol.* 1993;225:239-253.